NOISE PRODUCTION IN A TURBULENT BOUNDARY LAYER BY SMOOTH AND ROUGH SURFACES

Eugen Skudrzyk and Gillian Haddle
The Ordnance Research Laboratory
The Pennsylvania State University

* * * * *

The flow noise pressure produced in a turbulent boundary layer is proportional to the square of the fluctuations in turbulent velocity; consequently, it is also proportional to the coefficient of the drag and to the square of the free-stream velocity of the fluid. For a turbulent boundary layer, the coefficient of drag is practically independent of the Reynolds number and of the shape of the body. This property makes possible a general investigation of the boundary layer noise, without consideration of the shape of the body.

The flow noise turns out to consist of two components; one being due to the ordinary turbulence in the boundary layer, the other due to the small-scale turbulence generated by the surface roughnesses. At higher frequencies, the regular boundary layer noise seems to increase at a rate of 18 db, the roughness noise at a rate of 18 to 35 db per speed octave according to the density of the roughnesses. For plainly machined surfaces, roughness noise and boundary layer noise are equal at a frequency of 20 kc at about a speed of 20 knots. At higher speeds the roughness noise predominates over the boundary layer noise. If the diameter of the receiving hydrophone is halved, its flow noise sensitivity increases by approximately 12 db. A hydrophone mounted in the stagnation region of a streamlined body reads less flow noise at higher frequencies but more flow noise at lower frequencies than one mounted flush with the side walls of a streamlined body.

* * * * *

INTRODUCTION

Acoustic communication through the water medium is greatly handicapped by the noise produced by the moving vehicle and its machinery. At low speeds, the machinery noise seems to predominate over all other disturbances. But as the speed increases, the flow noise becomes greater until finally, at very high speeds, it seems to mask all other components of noise. The flow noise seems to be generated mainly in the boundary layer and in a turbulent boundary sublayer of the moving vehicle. The paper represents a first attempt to investigate theoretically and experimentally the component of flow noise produced by the surface roughnesses and the turbulence in the boundary layer of a body moving in water.

EXPERIMENTAL EQUIPMENT

To ensure well-defined experimental conditions, a boundary layer of constant thickness had to be generated. This regularity could be obtained with a rotating cylinder. There were reasons to believe that the finite length of the cylinder had little effect on the inner part of the boundary layer, which is known to be responsible for most of the flow noise, and that the results could be generalized later for any other curved surfaces.

The first experiments were made in the Ordnance Research Laboratory. It was certain that the properties of the cylinder walls would play an active part in the experiments. The fluctuating pressure could be expected to excite resonant modes; and the resonating modes would, in turn, excite the sound receiver, whether it was attached to the shell or placed far away from it. This complex behavior to be expected in any practical situation was the reason for leaving purely theoretical ground, for using the same hydrophones as are used with some in-service torpedoes, and for making up a cylinder of 1/8-inch steel, 17.9 inches outer diameter, and 24 inches long, with aluminum domes fastened on each end. The overall length was 42-3/4 inches (Fig. 1). It was driven by an 11.5-hp motor utilizing V-belts. Figure 2 shows the cylinder mounted in the acoustic water tank wherein all the measurements were taken. The sound receivers were two magnetostrictive hydrophones, one 2.5 inches in diameter, the other 5 inches in diameter. The hydrophones were mounted 180 degrees apart at the midpoint on the inside wall. Figure 3 shows the frequency responses of these hydrophones. The external-noise measurements were made with a similar receiver, a 24.5-kc hydrophone located one yard from the surface of the cylinder and at the same depth as the center of the cylinder.

The machinery noise is very small at high frequencies (as can be deduced from the curves for a smooth metal surface) - to be discussed later. The background noise may therefore be attributed to the structure-borne noise transmitted into the water tank, and to the thermal-noise level of the transducers. For small speeds the noise level equals the background noise level (-80 db below 1 dyne).

Other equipment was used in additional measurements performed in the Garfield Thomas Water Tunnel. The test section has a diameter of 48 inches. Each hydrophone was made up of two barium titanate discs, one inch in diameter, each 0.27 inches thick. One disc was fitted with a small hole in the middle of its face, that served to take up the lead to the hot electrode, which was at the interface between the two crystals. The unit was enclosed in a rigid brass box with a 1/16-inch thick membrane in front. Great care was taken to ensure perfect contact with the casing and between the crystals by using castor oil as a coupling agent. The unit was calibrated at the Black Moshannon Calibration Station. On the average its sensitivity was the same as the theoretical value of -100 db per bar re 1 volt. A second set of hydrophones of similar construction had a diameter of 1/2 inch, a thickness of 0.1 inch. Hydrophones were also mounted at the nose and at the side of a streamlined body having a maximum diameter of 4-1/8 inches and a length of 20 inches. This body was held in position in the middle of the test section of the channel by a strut. The frequency analysis was performed over the bands 250 to 500 cps, 500 cps to 1 kc, 1 kc to 2 kc, 2 kc to 4 kc, 4 kc to 8 kc, 8 kc to 10 kc, 10 kc to 15 kc, 20 kc to 25 kc, 30 kc to 40 kc, 60 kc to 80 kc, 80 kc to 100 kc, except for the results plotted in Fig. 16, which were obtained by a 5-cycle-band analysis.

THE VELOCITY DISTRIBUTION NEAR THE ROTATING CYLINDER AND IN THE TEST SECTION OF THE GARFIELD THOMAS WATER TUNNEL

The pressure distribution in the boundary layer of the rotating cylinder was measured with a multiple-rake manometer from a distance of 1/8 inch to about 6

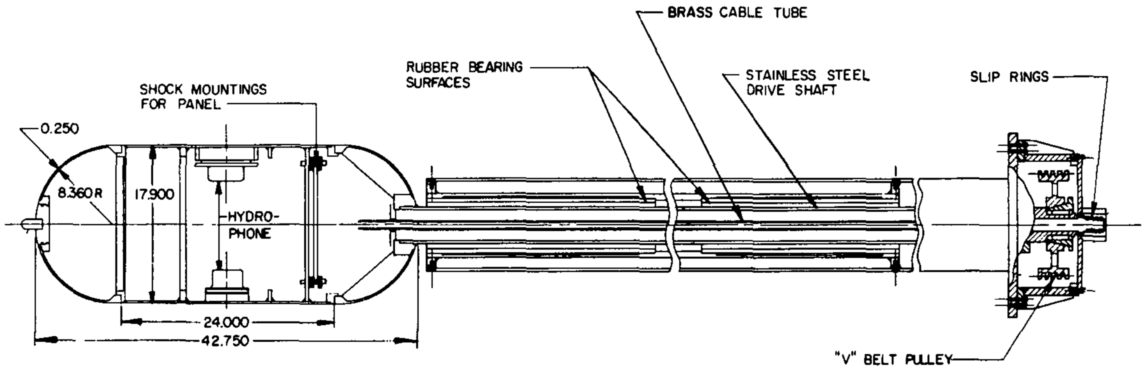

Fig. 1 - Rotating cylinder and drive shaft assembly

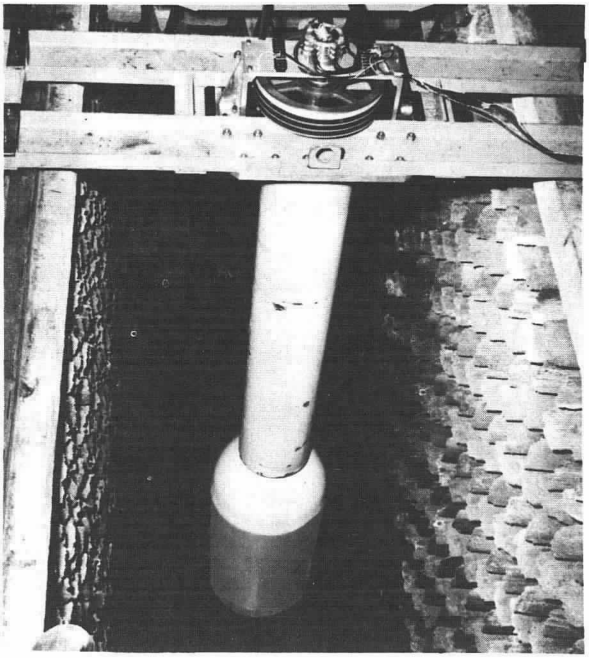

Fig. 2 - Rotating cylinder and tank

inches. The velocity distribution could then be computed. The measurements were in good agreement with the Prandtl von Kármán logarithmic-velocity formula (1) as shown in Fig. 4. For the plane of symmetry of the cylinder the following result was obtained:

$$\frac{u - u_o}{9.6} = 575 \log_{10} 960\ y + 25\ .$$

This unexpected result seems to be due to the fact that the shear velocity was very nearly constant over the whole boundary layer. It varied only by a factor of two from the innermost part of the boundary layer to the regions a few inches distant from the surface of the cylinder. This could be deduced from the drag measurements published by Theordorsen (2) and the value determined from the results represented in Fig. 4. A graph of the time variation of the pressure distribution (Fig. 5) proved that there was practically no time lapse between the surface speed of the cylinder and the building up of the inner regions of the boundary layer.

The velocity distribution over the major part of the cross section of the tunnel was uniform. Figure 6 shows the variation of the velocity over the boundary layer at sections 10 feet from the front end of the test section.

DERIVATION OF THE THEORY ON THE BASIS OF THE EXPERIMENTAL RESULTS

Whenever the Reynolds number of flow exceeds a limiting value, the flow becomes unstable and turbulent. This instability is caused by a predominance of the kinetic

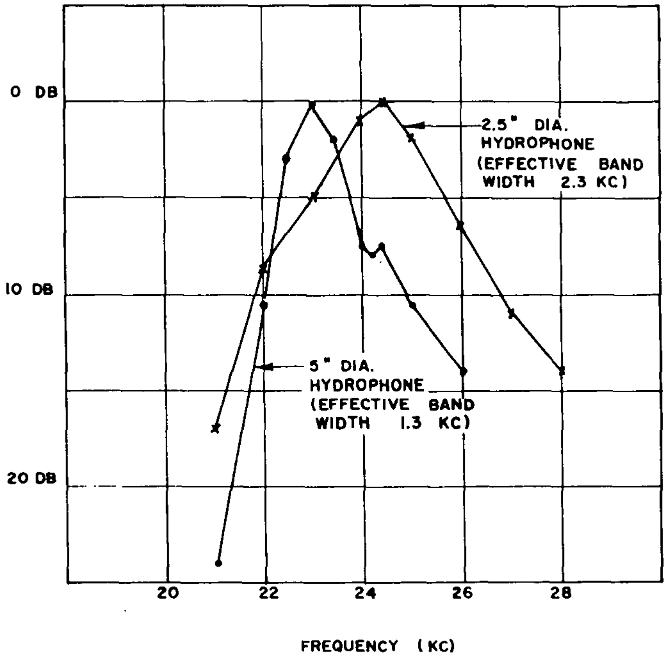

Fig. 3 - Hydrophone frequency responses

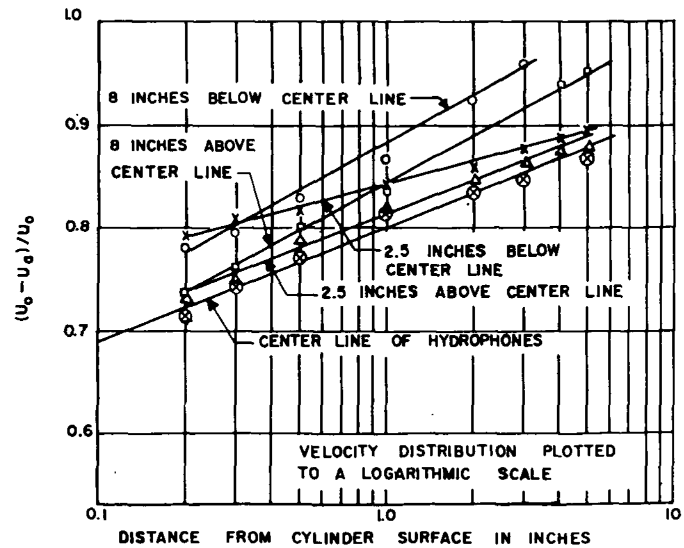

Fig. 4 - Mean velocity vs distance from surface of rotating cylinder

forces over the viscous forces. The kinetic forces such as the Kutta Jonkovsky lift and the Coriolis force are all proportional to the square of the velocity, whereas the frictional forces increase with only the first power of the velocity. At small Reynolds numbers, the velocity v is large in comparison to v^2 and friction governs the motion. Any disturbance in the velocity field therefore decreases rapidly to zero. At high speeds, v^2 is greater than v, and the kinetic forces determine the flow. Friction then becomes almost entirely negligible and the fluid behaves similar to an ideal gas or to a collection of ideal elastic balls. A disturbance introduced into the flow no longer decreases but persists or even increases with time, because of the production of mechanical energy by the surface drag.

The Reynolds number for which the kinetic forces become larger than the viscous forces can be crudely estimated. If we identify the disturbances with a cylindrical or, better, a spherical particle, a value of 50 to 100 is obtained, which agrees well with the experimental value 60 observed for the generation

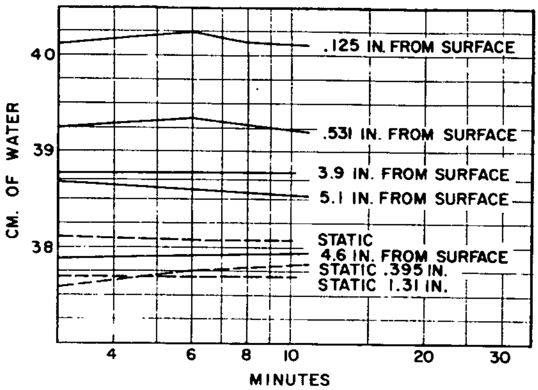

Fig. 5 - Radial velocity distribution as a function of the time after setting the cylinder in motion

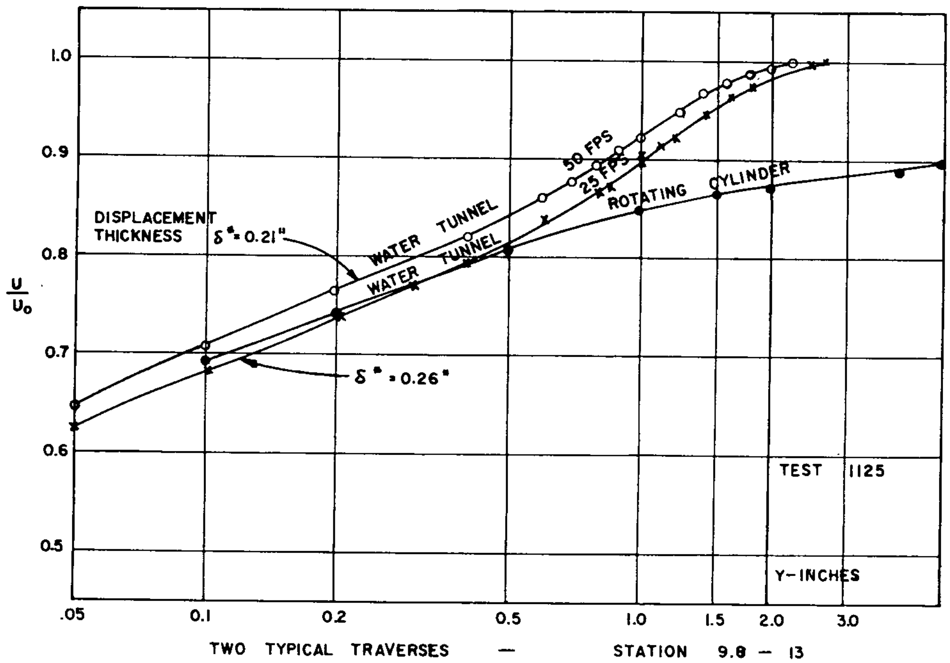

Fig. 6 - Tunnel velocity distribution over the boundary layer of the tunnel ten feet from the entrance end of the test section

of turbulence in a wake. The corresponding Reynolds number for the onset of turbulence in the boundary layer of the rigid body is at least 40 times as large. This signifies that the turbulence in the boundary layer of a rigid body is completely different in nature from the turbulence in a wake. This fact may be interpreted as follows: Because of the attractive forces exerted by the wall and the increased internal friction owing to the proximity of the wall, turbulence is much harder to start. Recent research (3) shows that turbulence is initiated by a phenomenon that is similar to a series of internal explosions of the fluid. But the moment turbulent patches or vortices have been formed, they possess so much kinetic energy that they may split up into smaller and smaller ones of less than 1/50th of the original diameter; and all these patches or vortices will still possess sufficient energy to have an appreciable lifetime ahead of them. The diameters of the vortices in the boundary layer of a rigid body therefore vary between a diameter equal to the thickness of the boundary layer and a diameter at least 40 times smaller; and the space-wave-number spectrum of this turbulence is continuously distributed over a fairly large volume in wave-number space. Under this condition, equilibrium laws such as the Kolmogorov laws (see Appendix A) for homogeneous turbulence may be expected to apply. In fact, it is possible to estimate the root-mean-square velocity fluctuation of the turbulence on the basis of this law, the result having at least the same order of magnitude as the measured values. Kraichnan (4a) has recently improved the Kolmogorov theory on the basis of statistical mechanics and has derived a slightly different wave-number dependency.

The velocity fluctuations caused by the turbulent patches increase the transportation of momentum and generate the drag. Our first task is to compute the magnitude of the velocity fluctuations, assuming the drag to be known. This computation can be performed in two different ways. We may start with the Stokes Navier equations. If the mean values of the components of the velocity are denoted by u_o, v_o, w_o, and the fluctuating velocity components are denoted by u', v', w', this equation becomes

$$\frac{\partial}{\partial y}\left(\bar{p} + \rho\overline{v'^2}\right) = \frac{\partial}{\partial y}\left(\mu\frac{\partial u_o}{\partial y} - \rho\overline{u'v'}\right).$$

The expression in the parentheses on the right-hand side represents the drag. Outside the laminar sublayer, the first term $\mu\ \partial u_o/\partial y$ is negligible; and the drag becomes

$$\tau = \rho u' v' .$$

The second method is based on the gas-kinetic considerations. Since friction is negligible at high Reynolds numbers, computing the drag in a similar manner is permissible, as the viscous force is gas-kinetics. The above expression is then re-obtained. If the flow is homogeneous, u' and v' are the same; but the turbulence in the boundary layer is not homogeneous. We may, however, define an effective velocity by the equation

$$v^{*2} = \overline{u' v'} .$$

This velocity v^* represents the geometric average of the fluctuating velocities, in the direction of the flow and perpendicular to the wall in the innermost part of the turbulent boundary layer at a distance from the wall, where the viscous forces just become negligible. According to the classical Prandtl theory of turbulence, v^* should be practically constant; according to the von Kármán theory, v^{*2} should decrease proportionally to the distance from the laminar sublayer to zero at the outer limit of the boundary layer, an assumption that agrees well with Laufer's (7) measurements. The magnitude of v^* determines the shear force near the wall, the so-called surface drag; it is known as the shear velocity.

The surface drag has been thoroughly studied for pipes (1,5) and channels (1,6) as well as for flat plates (1,6) and rotating cylinders (2). The experimental results show that the surface drag is approximately proportional to the square of the free-stream velocity u_o. The surface drag can therefore be expressed as the product of the coefficient of drag c_D and the square of the free-stream velocity:

$$\tau = C_D \cdot \frac{1}{2} \rho v^{*2}$$

ρ denoting the density of the fluid.

This coefficient of drag proves to be practically a constant and to be equal to 3×10^{-3} whenever the flow is turbulent. It changes by only a factor of 3 when the velocity is changed by as much as a factor of 5000 (Ref. 1). Since this surface drag is generated in the inner part of the boundary layer, we may expect that it will not greatly depend on the curvature of the surface nor on the size of the body that generated it. This conclusion has been verified by Theodorsen (2) for a series of rotating cylinders. The ratio of the height to the diameter has been varied by as much as a factor of 20. Nevertheless, all the measured points seem to lie on the same curve (Fig. 7). We may therefore assume that the coefficient of drag is independent of the curvature and of the size and shape of the body. This approach means a considerable simplification in the study of flow noise.

The fluctuating velocity v^* can be computed by equating the theoretical and experimental results.

$$\rho v^{*2} = \frac{1}{2} C_D \rho u_o^2 = 15.10^{-4} \rho u_o^2 \quad \text{or} \quad v^* = 0.04 \ u_o .$$

The effective velocity then turns out to be very nearly equal to 4 percent of the free-stream velocity.

This result is in good agreement with Laufer's channel measurements (7). The shear velocity reaches 4 percent at the outside of the laminar sublayer, and then decreases linearly with the distance until it becomes zero at the outer side of the boundary layer. Laufer's measurements also show that u' is about 8 percent of u_o, and v' slightly less than 4 percent of u_o; because of the imperfect correlation between these two, $u' v'$ is only 4 percent of u_o.

The next task is to derive the connection between the fluctuating velocity v^* and the pressure at a point in the boundary layer. The boundary layer is usually thin and the scale of the turbulence we are interested in small in comparison to the acoustic wavelength. Because of this fact the pressure fluctuations in the boundary layer will be primarily kinetic. They are generated by the centrifugal and similar forces of the rotating vortices; they represent the near field of the dipole, quadrupole, and octupole sources that mathematically describe the turbulence. To distinguish these pressure fluctuations from a true sound field, they are usually summarized under the name quasi sound. In addition to this quasi sound, true sound that is radiated off to greater distance is produced because of the unsteadiness of the flow. But this true sound seems to be negligible in the boundary layer in comparison to the internal near field generated by the rotating vortices. This fact makes it possible to establish the connection between the fluctuating velocity and the sound pressure by an equation of the type of the Bernoulli equation (Appendix B) with a slightly modified constant

$$p = \alpha \rho v^{*2} ,$$

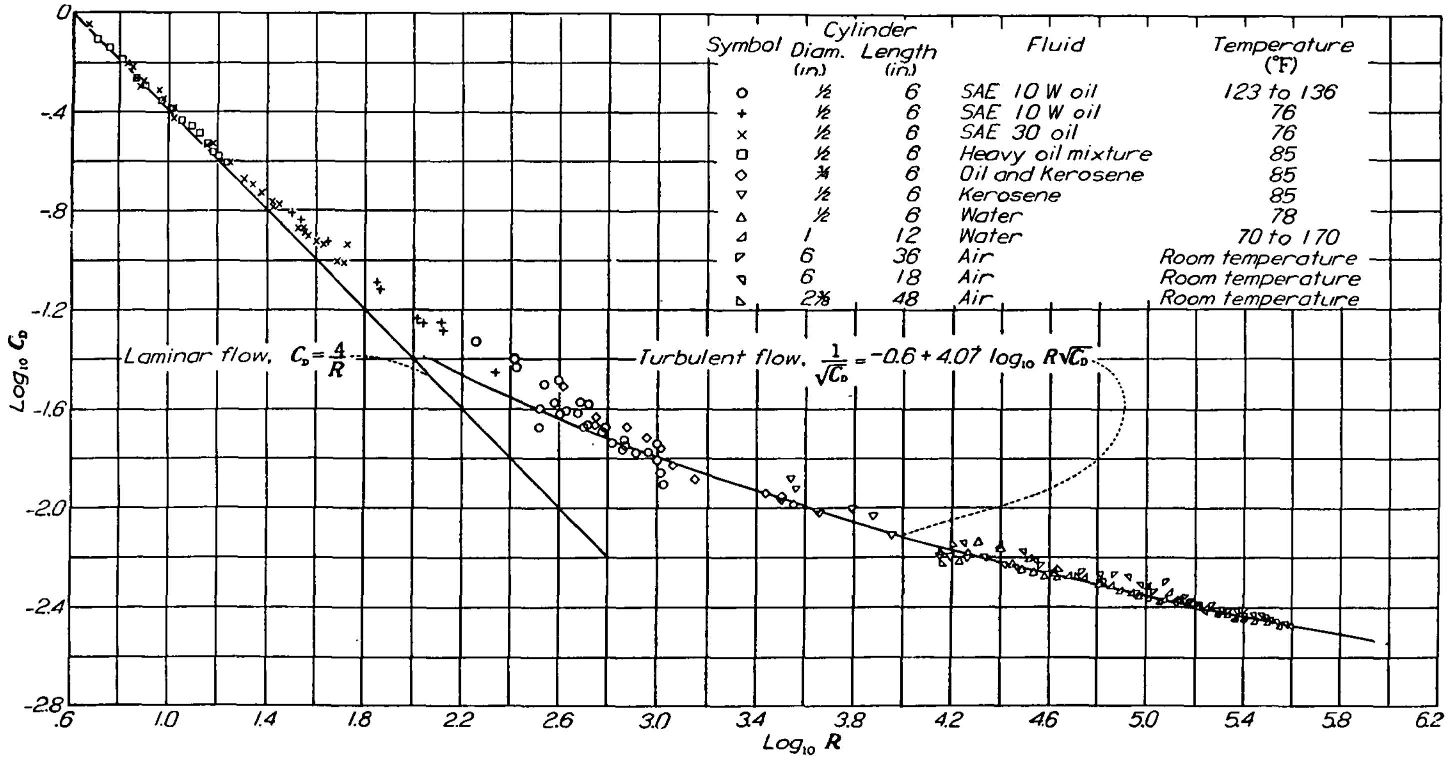

Fig. 7 - Drag coefficient C_D for rotating cylinders as function of Reynolds number

where α is a constant of the order of magnitude one. This quasi sound pressure would be actually measured, if the sound receiver were infinitely small.

A receiver of finite size measures the average value of the pressure over its sensitive area. This average value is the smaller, the larger the area, since the pressure maxima and minima compensate one another. If the hydrophone area is very large in comparison to the scale of the turbulence, the average quasi sound pressure will be very small, and the hydrophone reading will be mainly determined by the true radiation field generated in the whole space that surrounds the hydrophone. The above formula will then no longer apply.

Let us consider a practical case, such as a vehicle traveling with a velocity of 20 knots or 10 meters per second. The effective fluctuating velocity would be 40 centimeters, and the noise pressure as given by the above equation would be 1600 dynes/cm^2. This result is very interesting, but it does not yet give any information about the flow noise actually produced by the moving body. The frequency spectrum is still unknown. The flow noise spectrum may be centered at extremely low frequencies and be inaudible, or may be in the audible or supersonic range.

First of all, we have to find the connection between the frequency spectrum of the noise pressure and the scale of the turbulence. We may identify the patches with the maxima and minima in a progressive wave that moves with the local mean speed $\bar{u}$ of the flow along the surface of the receiving hydrophone. This local speed $\bar{u}$ varies according to how far away from the laminar sublayer the patches are between u_o and v^*. The pressure fluctuations as recorded by the hydrophone will then have a frequency

$$f = \bar{u}/\delta ,$$

where δ is the distance between successive vortices or is the scale (the effective diameter) of the turbulent patches. For low-frequency noise, this local velocity $\bar{u}$ will have to be assumed to be roughly equal to the free-stream velocity of the fluid.

There are two possible ways to compute the frequency spectrum of the flow noise. Kraichnan (4c) assumed a Gaussian correlation function for the velocity correlation, his supposition being equivalent to assuming a Gaussian energy spectrum of the turbulence. The pressure spectrum is then derived by a series of integrations. The result still resembles a Gaussian spectral distribution in its sharp cutoff at frequencies above a limiting frequency represented by

$$f = u_o/\delta ,$$

where δ is the thickness of the boundary layer. If we substitute numerical values and assume a speed of 20 knots or 10 meters per second and a thickness of 1 centimeter for the boundary layer, this frequency will be 1 kc.

The second procedure is as follows: We may divide the spectrum into a low-frequency spectrum and a high-frequency spectrum. For the derivation of the low-frequency spectrum, the patch of turbulence may be considered as equivalent to a pulse of a width equal to the diameter of this patch. If we assume this diameter to be roughly equal to the thickness of the boundary layer, the spectrum then turns out to be constant up to a space wavelength equal to the diameter of the patch or to the thickness of the boundary layer. From there on it decreases as $(\sin x)/x$. For the derivation of the high-frequency part of the spectrum, the details are furnished at least approximately by the equilibrium laws of turbulence. The Kolmogorov law, for instance, predicts that at high frequencies the energy spectrum decreases inversely as the 3/2 power of the space wavelength. The spectral density of the turbulence noise may thus be expected to be approximately constant at lower frequencies up to the frequency u_0/δ determined by the ratio of the free-stream velocity to the thickness of the boundary layer. From there on, it may be expected to decrease approximately inversely as the 3/2 power of the scale of the turbulence or the space-wave number.*

Figure 8 shows some measurements performed in the Garfield Thomas Water Tunnel at State College. The method used in making these measurements will be described later. The noise level is shown as a function of frequency for several flow speeds. Up to a certain frequency, which in this particular case should be about 400 cycles per second, the noise level should be constant; and from there on should approximately decrease inversely as the 5/3 power of the frequency.

The experimental results show that we must distinguish between two types of flow noise. The first type is the one we just discussed: it is the flow noise produced by the velocity fluctuation in the turbulent boundary layer that has been studied thoroughly, in great detail, and very ingeniously by R. H. Kraichnan (4b). M. Harrison (8) verified the predictions of the Kraichnan theory experimentally in air-channel flow and proved that the assumptions in Kraichnan's work are indeed very reasonable.

The second component of flow noise is produced by the surface roughness. With an increasing speed of flow, the laminar boundary layer becomes continuously thinner. When the velocity reaches a certain value, the roughnesses become greater than the thickness of the laminar boundary sublayer and penetrate the laminar boundary sublayer. They then become capable of shedding vortices or of producing a von Kármán vortex street (9). The vortices generated this way increase the surface drag and create a turbulent sublayer on top of the laminar boundary sublayer. Because of its small scale and its great energy content, this turbulence may be expected to create a high noise level with an essentially high-frequency spectrum. Before going more into detail, let us prove that this "roughness noise" does indeed exist. Figure 9 shows measurements that have been performed with the aid of a rotating cylinder 42 inches high and about 23 inches in diameter, and with a microphone mounted flush with the wall of the cylinder. The abscissa in this figure represents the surface velocity of the cylinder; the ordinate represents the noise level. Let us first concentrate on the measurements performed with a smooth painted cylinder surface, a surface as smooth as possible. Until the speed exceeds a certain value, the noise level is that of the ambient noise; from there on, it increases at a rate of roughly 18 db per speed octave, as for true boundary layer noise. Now let us consider a second measurement that has been performed under the same conditions except that the surface of the cylinder has been roughened (grit 180). The noise level now exceeds that of the ambient noise at a much slower speed than in the previous case. For the same velocities the flow noise produced by the rough surface is 20 to 50 db greater than that produced by the smooth painted surface. Since nothing else has been changed, this greater noise must be attributed to the effect of the surface roughnesses. There is thus no doubt that roughnesses generate flow noise.

The effect of surface roughnesses on the drag has been thoroughly studied in the literature for flat plates (1), pipes (1,5,6), and a rotating cylinder (2). The results are always the same. Whenever the surface roughnesses penetrate the laminar boundary sublayer, they increase the surface drag. The theory shows that the roughnesses

*It can be shown that the high-frequency part of the spectrum of the squared function is approximately proportional to the spectrum of the original function at half the frequency, if the latter is a randomly varying statistical function, and that it is accurately proportional to it, if the original function has a Kolmogorov-type spectrum.

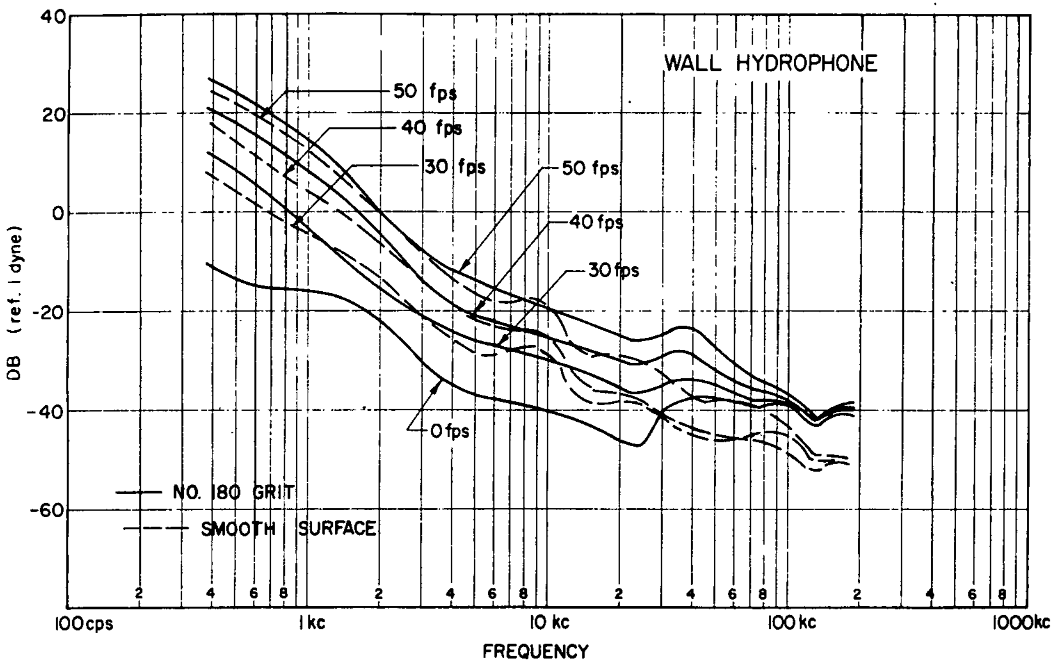

Fig. 8 - Spectrum (half-octave measurements) of the boundary layer noise in the test section of the Garfield Thomas Water Tunnel for various water speeds

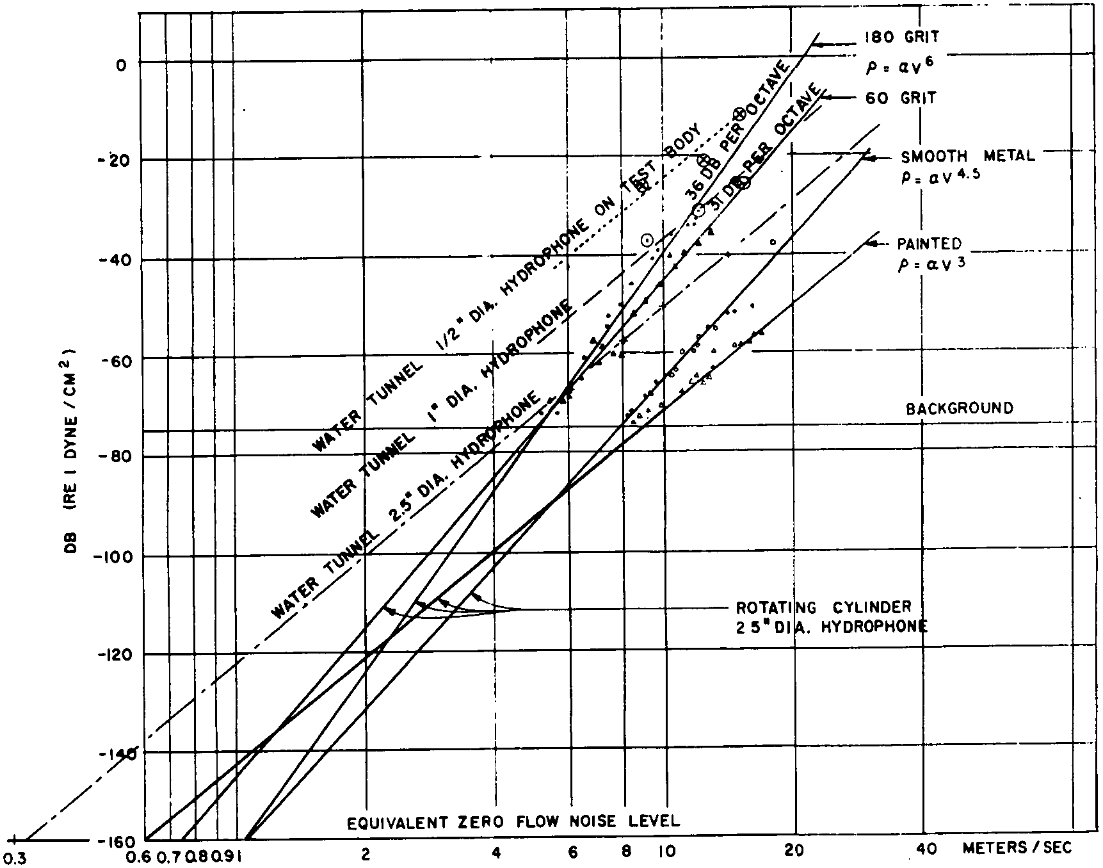

Fig. 9 - Noise level as a function of speed and surface conditions as measured with the the 7.5-in.-diameter hydrophone in the rotating cylinder

become larger than the thickness of the boundary sublayer if their Reynolds number becomes greater than 5:

$$5 \leq \frac{hv^*}{\nu} .$$

The velocity in the immediate vicinity of the laminar sublayer is approximately equal to the shear velocity. The above Reynolds number had therefore to be formed with the height of the roughnesses and the shear velocity.

With the aid of the previous results, the above Reynolds number of 5 can be expressed as a function of the free-stream velocity. The roughnesses are then found to become effective when the speed is greater than the critical value given by

$$v_{crit} = 10^{-2}/h \text{ (knots)} ,$$

where h is the height of the roughnesses in inches. An analogous condition can be derived for the shedding of vortices by roughnesses in a nonturbulent boundary layer; the Reynolds number then has to be formed, with the height of the roughnesses and the laminar velocity at a distance h from the walls. This Reynolds number increases toward the stagnation point, as would be expected because of the greater velocity gradients. For roughnesses of 10^{-2} inch and a distance from the edge of the body greater than a few centimeters numerically, very nearly the same results are derived for the roughness noise; and it should make little difference whether the bulk of the boundary layer is turbulent or laminar. However, the regular boundary layer noise will not be generated in the stagnation region because of its predominant laminar nature. It is hard to predict the reduction of flow noise that could be expected in such a case because flow noise will also be radiated back from the other parts of the moving surface into the stagnated area.

Figure 10 illustrates the above results for rotating cylinders covered with roughness of various grain sizes. Whenever the Reynolds number of the roughnesses exceeds 5, the drag becomes greater than that for a smooth surface. The speed at which these increases are observed is thus a function of the height of the roughnesses only, but the magnitude of the increase of the drag is a function of the density of the roughnesses. This is illustrated in Fig. 11, which represents measurements where the density of the roughnesses has been varied.

The noise pressure has been shown to be proportional to the drag. The increase in drag because of the small-scale surface roughnesses may therefore be expected to show up in a corresponding increase of high-frequency flow noise. That this assumption is essentially correct is illustrated in Fig. 9. No flow noise can be observed at lesser speeds. At the critical Reynolds number, flow noise may be expected to be generated, but the intensity of this noise is still so small that it is completely masked by the ambient noise. From a certain speed onwards, a speed that depends on the size and density distribution of the surface roughnesses, the level of the flow noise exceeds that of the ambient noise; it increases at a rate of 18 to 35 db per speed octave, according to whether the surface is rough or smooth.

For grit 180, 80 percent of the particles have a height of about 5×10^{-3} inch. The critical speed is therefore 2 knots or 1.08 m/sec. If we extrapolate the curve for this kind of grit down to a speed of 2 knots, from whence the roughnesses would be expected to become acoustically effective, the noise level turns out to be -158 db. This value may be considered as the equivalent of zero flow noise level for the condition of the experiment. The other curves should then intersect with the "zero flow

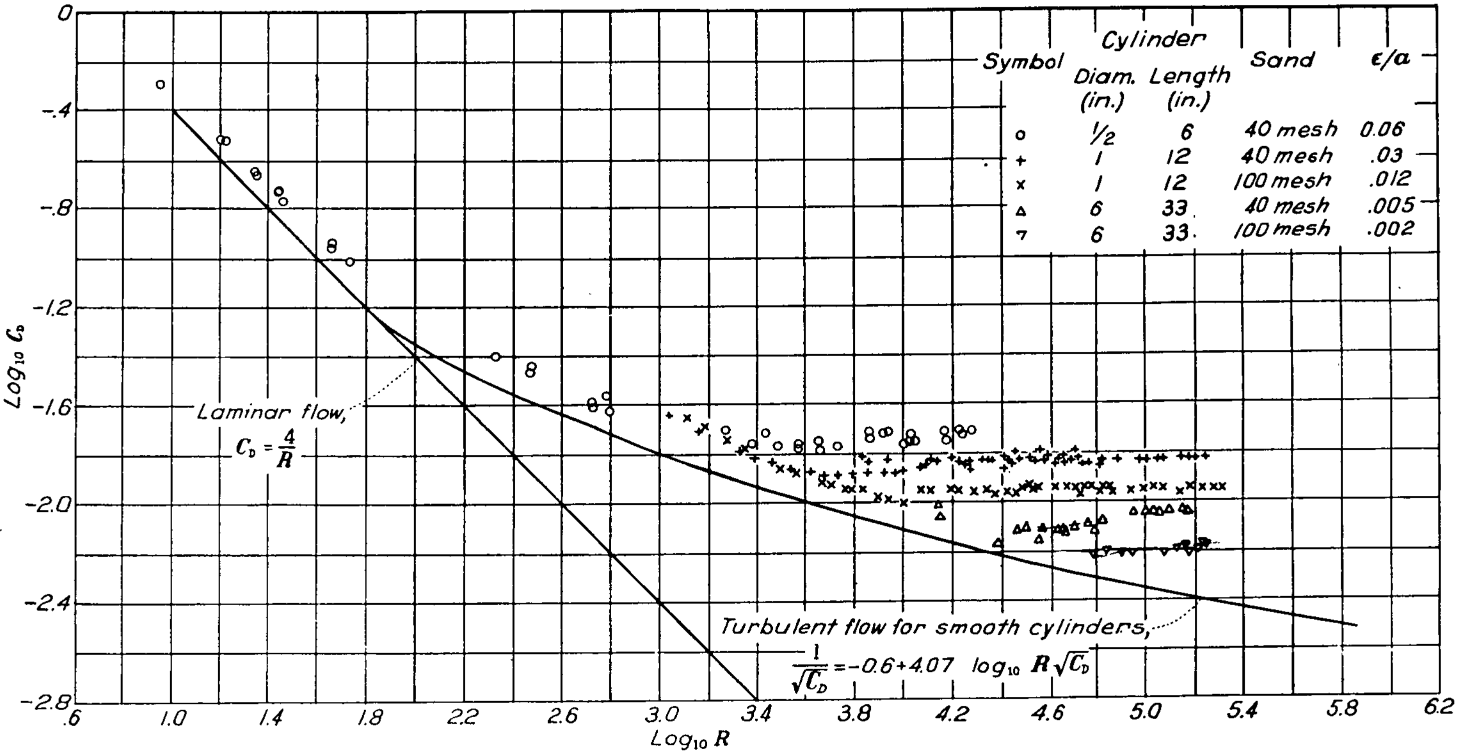

Fig. 10 - Effect of surface roughness, or grain size, on the drag coefficient in the case of saturation density of particles (From Ref. 2)

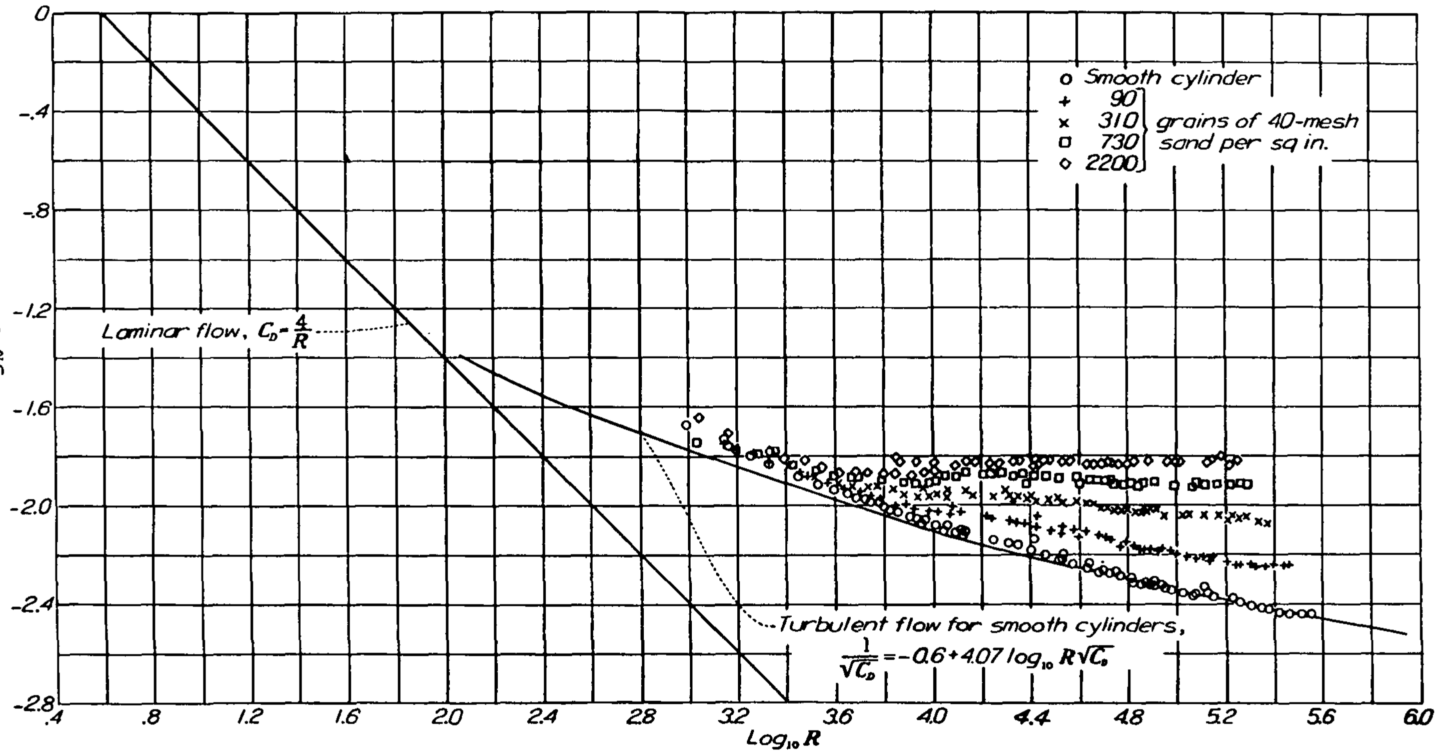

Fig. 11 - Effect of varying density of surface roughness on the drag coefficient (From Ref. 2)

noise" level - 158 db at speeds equal to the corresponding critical values; and this indeed seems to be what happens if we allow for a small experimental error and for the fact that the energy of the background and that of the flow noise add up to the resultant noise level and change the shape of the curves at lower noise levels. Grit 60 exhibits maximum dimensions of 10^{-2} inch (v_{crit} = 1 knot). The corresponding critical speed is therefore 0.54 m/sec. The measured line intersects very nearly at the point $v = v_{crit}$ 0.70 m/sec with the equivalent zero flow-noise level at -159 db. For a smooth machine-polished metal surface, v_{crit} = 0.75 m/sec (1.5 knots). Paint seems to cover the smaller roughnesses and appears to increase the larger-size roughnesses with paint streaks so that the corresponding v_{crit} is 0.5 m/sec (1 knot). The extrapolation of the measurements to levels considerably below the ambient noise level is, of course, thoroughly hypothetical; and the assumption of a zero effective or equivalent flow noise level is likewise tenuous.* But this assumption seems to represent a working assumption that is borne out by the experimental results, at least as long as no detailed theory is available.

Like the slope of the curves for the drag, the slope of the noise curves is also a function of the density distribution of the roughnesses. The noise level increases linearly with the logarithm of the speed by 18 db per octave of increase in speed if the surface is very smooth and by up to 35 db per octave increase in speed if the surface is rough. The flow noise generated by a surface with small but densely distributed roughnesses may thus exceed the ambient noise level at much slower speeds than that generated by a surface with large roughnesses if the density of the large roughness is sufficiently small. The noise levels have been measured simultaneously with two hydrophones, one 2.5 inches in diameter, the other 5 inches. The results are identical except for a constant difference in level, the smaller hydrophone being more sensitive by 10 - 13 db (Fig. 12). These results show the average pressure over the hydrophone area that determines the hydrophone reading and the compensation of the pressure maxima and minima over the area of the hydrophone. This average pressure is greater, the smaller the diameter of the hydrophone.

One of the most puzzling results of these investigations was the fact that the noise level measured with a similar hydrophone outside the boundary layer at a distance of one yard proved to be approximately the same as that measured in the boundary layer (Fig. 13). This result can be explained again as a consequence of the compensation of the pressure maxima and minima. The hydrophone used did not indicate the true pressure fluctuations in the boundary layer, but the average value over an area of a diameter of about the magnitude of the acoustical wavelength. On the basis of diffraction theory, it can be shown that the pressure at a certain distance from the source distribution can be computed as a function of the pressure at the boundary surface. In this computation the average value of the pressure for an area roughly equal to the square of the wavelengths determines the result, and this is exactly the quantity that was responsible for the hydrophone reading inside the boundary layer. This result shows that in the presence of flow noise a small hydrophone will always be a poorer sound receiver than a large one.

Damping the shell by coating it internally with a damping varnish had only a small effect on the measured levels (Fig. 12). This result might be expected. At high frequencies, the resonances of the shell overlap to a continuous background, and individual resonances do not greatly contribute to the result.

*It is hardly worthwhile to try to improve the quality of the extrapolation by assuming the noise level to be proportional to a power of the velocity difference ($v - v_{crit}$) since v_{crit} usually is small in comparison to v.

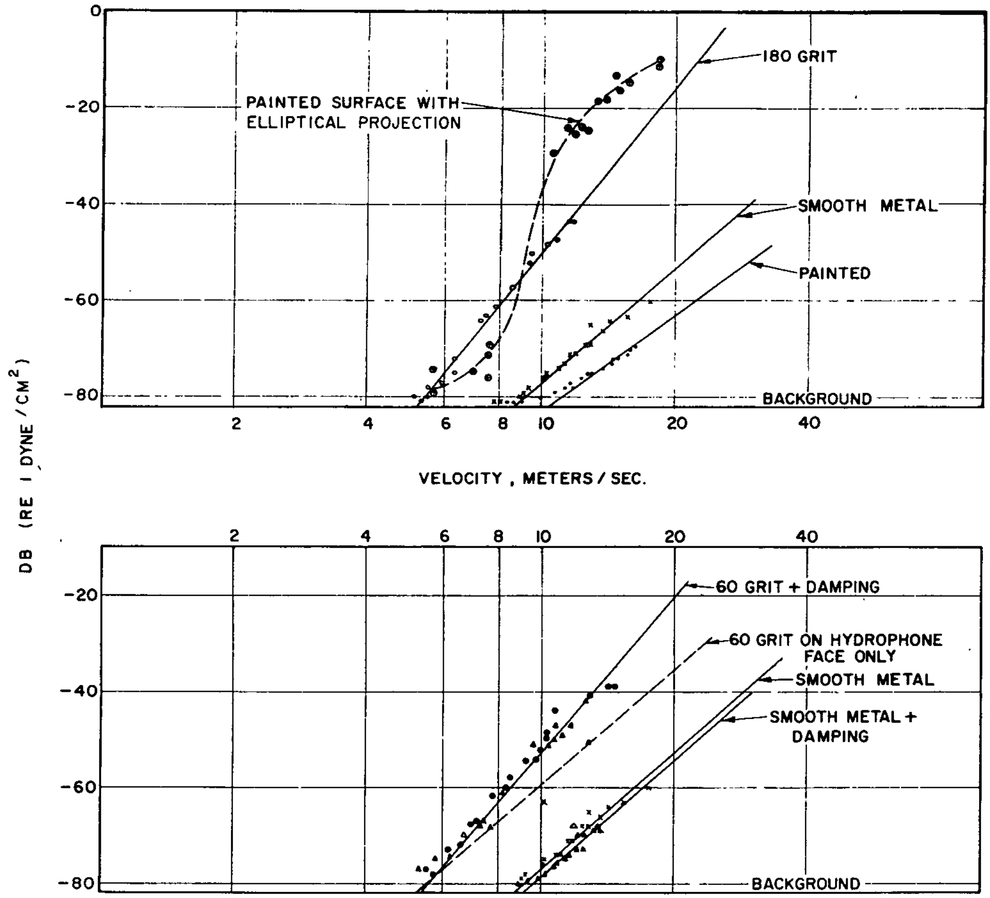

Fig. 12 - Internal noise level as measured with the five-inch-diameter hydrophone and the effect of damping and of a large elliptical projection on the internal noise level

Figure 14 shows some measurements performed in the Garfield Thomas Water Tunnel* with a microphone mounted on a very smooth laminar-flow-noise head. The roughnesses are relatively large, but not numerous. The slope is 18 db per octave speed change, as would be expected for true boundary layer noise.

A number of flow noise measurements on ships have been reported for which the slopes are 18 to 22 db per speed octave, but the absolute levels are larger by 10 to 20 db than those found in the measurements obtained by using the cylinder. This means that in practical cases the roughnesses generating the flow noise are usually relatively large, but few in number.

The cylinder measurements lead to a rough estimate of the noise level as a function of the speed, the size, and the density of the roughnesses. The experimental results can be expressed as

*This curve has been measured by J. H. McGinly, ORL

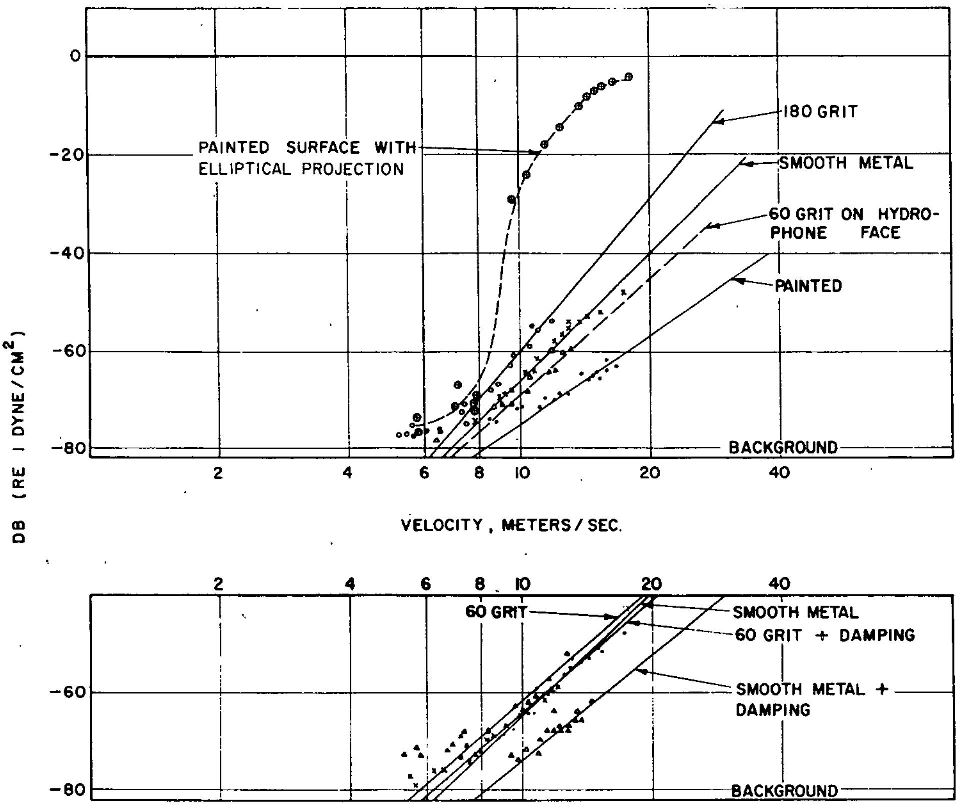

Fig. 13 - External noise at one meter from the cylinder surface for differently treated surfaces

$$p = -158 + \alpha Q \text{ decibels}$$

for the 2.5-inch-diameter hydrophone as receiver, where α is a factor varying between 20 and 25 db per octave of speed change, according to whether the surface is smooth and painted and the roughnesses scarce, or completely rough as when treated with grit. Since Q represents the number of octaves above the critical speed,

$$Q = \log_2 \frac{v}{v_{crit}} .$$

The experimental results can then be summarized. The flow noise level at 25 kc measured with a hydrophone of a diameter of 2.5 inches and a bandwidth of 2 kc attains -80 db below 1 dyne per centimeter square (spectral level, per cycle), when the speed is 20 times the critical speed if the surface is smooth (carefully painted) or 5 times the critical speed if the surface roughnesses are densely distributed (as for instance in the case of a grit-covered surface). The noise level then increases at a rate of 20 db per octave of increase in speed if the surface is smooth (roughnesses widely distributed) or at 35 db per octave of increase in speed if the surface is completely covered with roughnesses. This means that for a vehicle traveling at a speed of 50 knots, the critical speed has to be at least 8 knots. The roughnesses then have

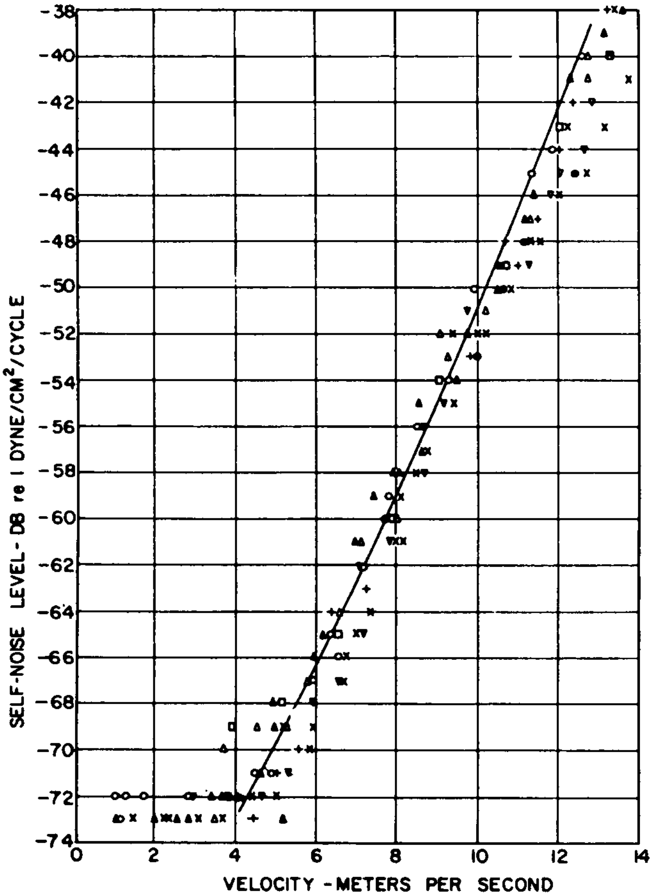

Fig. 14 - Flow noise level in the Garfield Thomas Water Tunnel

to be smaller than 1.25×10^{-3} inch. Such a vehicle will then generate no audible roughness noise.

To gain additional information about flow noise, measurements were performed in the boundary layer at the Garfield Thomas Water Tunnel. Four hydrophones were mounted flush with the walls of the Tunnel and two hydrophones were mounted in the streamlined body in the middle of the tunnel, one hydrophone at its nose and the other at its side. Figure 8 which shows the results measured with the hydrophone flush with the wall of the Tunnel has already been discussed in connection with the speed frequency spectrum of flow noise. Figure 15 shows the measurements with the hydrophones mounted on the streamlined body. The noise level received by the nose hydrophone at frequencies between 500 cps and 20 kc is 5 to 20 db smaller than that recorded by the side hydrophone. But at low frequencies the picture reverses. The nose hydrophone receives considerably more flow noise than the side hydrophone. This is very apparent when listening to tape recordings. The noise received with the stagnating hydrophone sounds bubbly and seems to be very rich in low frequencies;

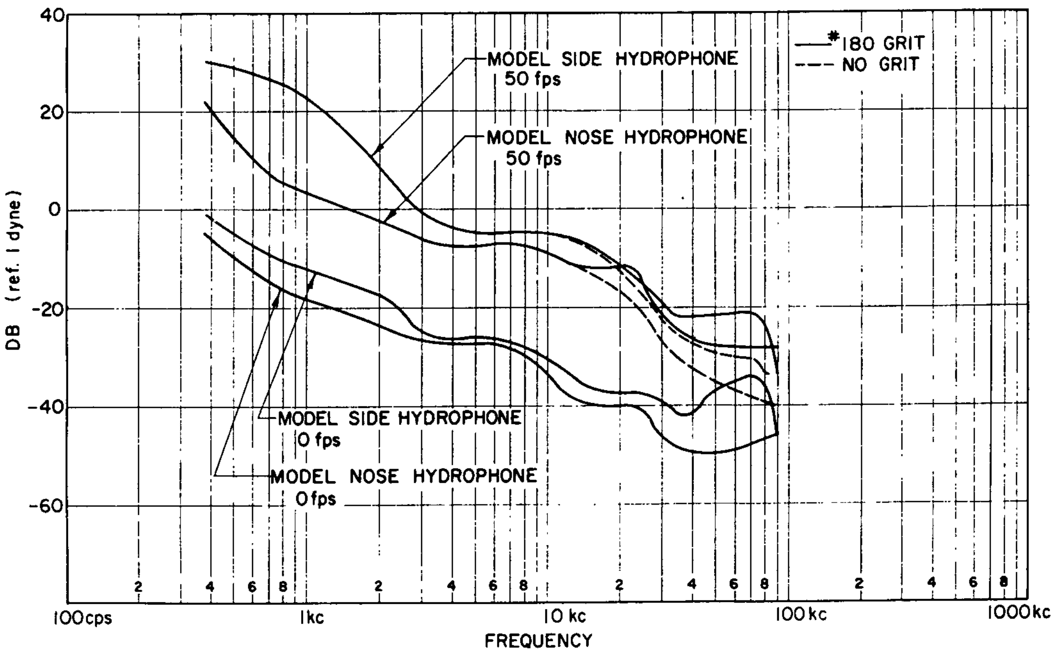

Fig. 15 - Measurements with two hydrophones mounted flush with nose and side wall of a streamlined body

the higher frequencies are almost completely masked. The noise received by the side hydrophone resembles more a hissing sound with very small low-frequency contents. This phenomenon can be traced through all recordings. This low-frequency sound received by the stagnating hydrophone seems to be due to the stagnation pressure generated by the larger-scale turbulence that hits its sensitive area. The smaller-scale turbulence does not seem to produce a similar effect; it is very likely that this turbulence is damped out entirely by the stagnation of the flow. Figure 16 shows a narrowband analysis of a second series of such measurements.

The boundary layer noise in the Garfield Thomas Water Tunnel is relatively large. But the effect of different shapes of test vehicles and of the position of the hydrophones could still be investigated if these objects were densely covered with coarse grit and if the speed of the flow were sufficiently high. Preliminary measurements performed on grit-covered surfaces (grit 180) and surfaces covered with a resilient coating did not yet lead to new results (Fig. 17), since the grain size of the

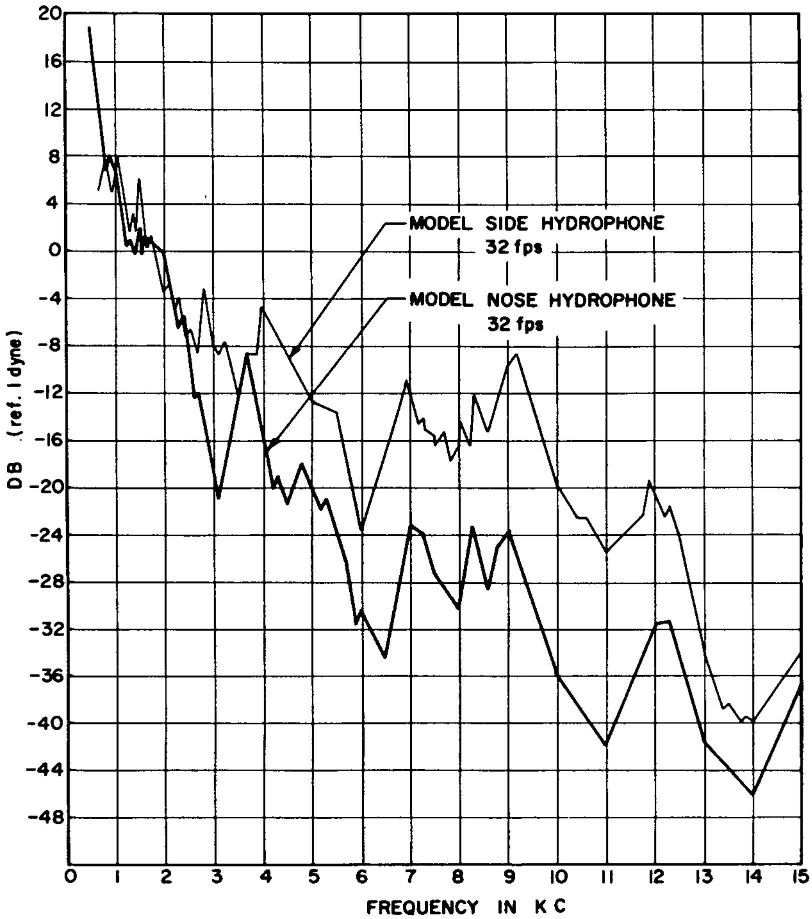

Fig. 16 - Narrow-Band frequency analysis for nose and side hydrophone on streamlined body

grit and the speed of the flow (50 ft/sec) still were too low. But there seems to be little doubt that proper treatment of the surfaces and the use of greater flow velocities will make possible detailed flow-noise studies in such a channel.

RELIABILITY OF THE MEASUREMENTS

To test the reliability of the results, all the measurements were repeated five months later. Identical results were obtained. Special tests have been made to ensure that cavitation did not interfere with the measurements.

Cavitation usually starts at a certain speed, increases the noise almost abruptly to a high value, and then for a time remains almost constant; later, it even decreases again. The dashed curve in Fig. 13 is an example of a case where cavitation was produced intentionally by welding a projection shaped as a semi-ellipse (6 inches long, 4 inches high, and 1/4 inch thick) to the cylinder surface at the height of the hydrophone. The moment cavitation starts, the noise intensity jumps quite suddenly by almost 60 db. In spite of the relatively large size of the projection, cavitation is seen to take place only at speeds above 7 meters per second. Typical for the measurement was a continuous fluctuation of the noise level around a mean value.

Another proof that cavitation did not interfere with the measurements is given by a curve in Fig. 12 for which the area of the larger hydrophone was covered with grit. The noise level is much greater than that of the painted surface, being almost exactly the same at the untreated hydrophone area, if its 10-db greater sensitivity to incoherent flow noise is taken into account. Cavitation would have affected the response of the first hydrophone to a much greater extent than that of the second, 17 inches distant from the first and in the sound shadow.

During the measurements performed in the water tunnel, cavitation could be easily identified by increasing the pressure. The unsteadiness of the noise (like a series of explosions) makes recognition of this phenomenon very easy.

The noise level owing to extraneous noise would be expected to increase continuously with a relatively low power of the speed; and it would be independent of the conditions of the surface of the cylinder. Extraneous noise could not have affected the rough-surface measurements of the cylinder, but very likely it also had no effect on the results for the smooth and the painted surfaces.

SUPPLEMENTARY WORK

The study described above represents an attempt to derive a general understanding of the features of flow noise. The measurements in the Water Tunnel will be repeated in the near future with more sensitive hydrophones and with hydrophones of variable area. Work with buoyant units has been taken up, and the field program has just started at Key West to supplement and to verify the previous conclusions. A paper submitted to the Journal of the Acoustical Society contains the experimental data described above and theoretical derivations performed since the Flow Noise Symposium. This paper contains a quantitative analysis of the near-field component and of the flow-noise component radiated to greater distances. The high-frequency boundary-layer noise pressure turns out to be inversely proportional to the thickness of the boundary layer, a relation which is in agreement with the derivations published in the literature and the experimental results of M. Harrison (8). Because of the large thickness of the boundary layer of the rotating cylinder, the boundary-layer component of flow noise is relatively weak, and roughness noise shows up at considerably

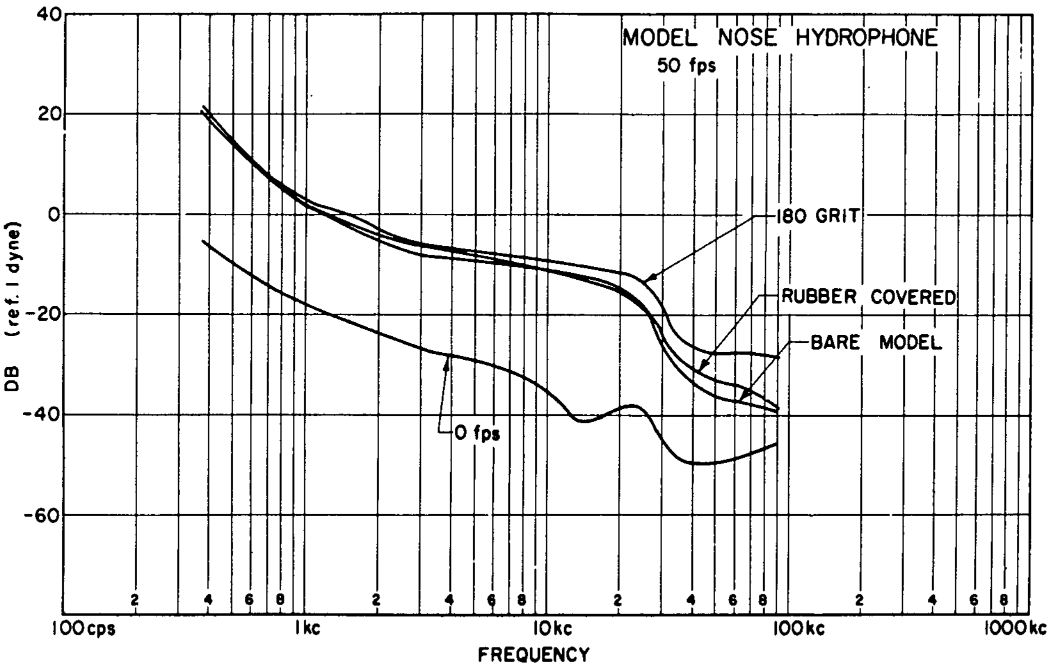

Fig. 17 - The effect of grit and a pressure resilient coating on flow noise. The velocity of the flow and the size of the roughnesses are not yet sufficiently large to mask the tunnel boundary layer noise.

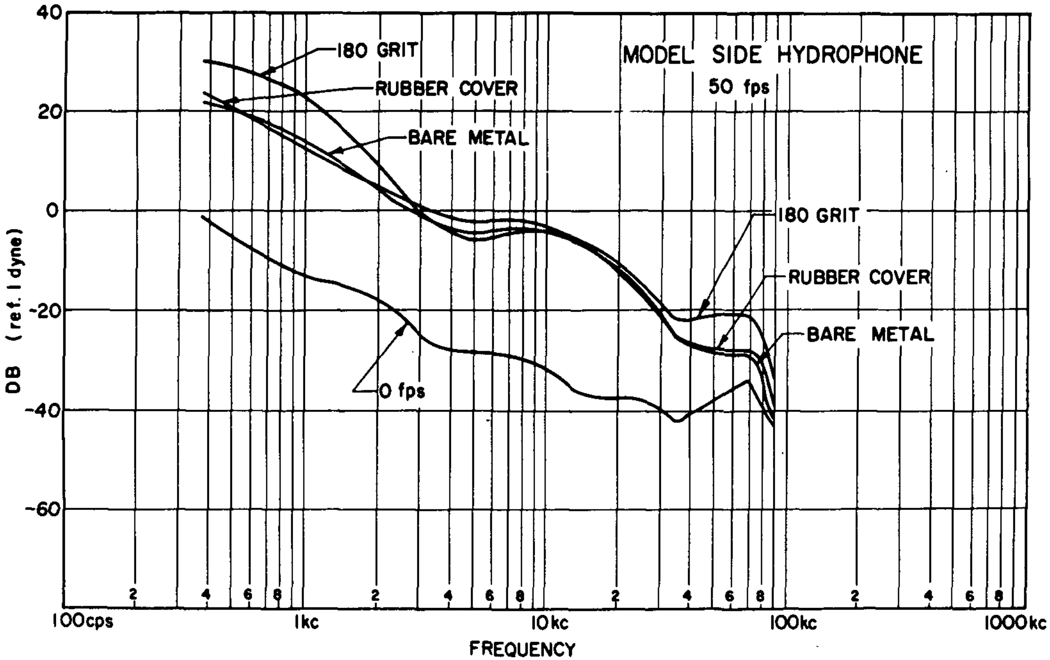

Fig. 17 (Continued) - The effect of grit and a pressure resilient coating on flow noise. The velocity of the flow and the size of the roughnesses are not yet sufficiently large to mask the tunnel boundary layer noise.

lower velocities in the case of the rotating cylinder than in other cases. In the Garfield Thomas Water Tunnel, the boundary layer noise is so intense that roughness noise shows up only at speeds above 40 ft/sec. This situation seems to indicate that in the case of ships and similar vehicles, boundary layer noise will be predominant, on the average, at speeds below 20 knots, whereas at speeds above 20 knots, the noise produced by the surface roughnesses will usually determine the noise level.

ACKNOWLEDGMENTS

The cylinder method for measuring flow noise was proposed by J. D. Weir, the equipment designed by H. F. Wagener, and the studies were initiated by F. P. Finlon. The velocity-distribution measurements were performed by T. E. Pierce and the personnel at the Garfield Thomas Water Tunnel. The authors wish to thank Dr. G. F. Wislicenus for valuable discussions and for his cooperation in the Water Tunnel. They also wish to thank R. J. Urick for the stimulus he provided, and to acknowledge the cooperation of Frank Kaprocki in the frequency analysis, and that of Ed Ulrich in assisting with design problems.

Appendix A

THE EQUILIBRIUM LAW AND THE STATISTICAL BEHAVIOR OF DYNAMIC DISTRIBUTION

Many of the statistical phenomena that nature exhibits are produced by or have originally been produced by reservoirs of energy feeding into a dynamic system that redistributes and eventually absorbs the energy store by increasing the entropy of the system. This is the course followed by the turbulence generated in the boundary layer of a moving body, where the original energy is given by the kinetic energy of the flow. The same course accounts for the turbulent motion of water in the sea or the air above the ground, where the primary energy is supplied by the radiation of the sun, and for the surface waves of the sea, where the wind furnishes this energy.

This equilibrium law can be derived on the basis of simple dimensional considerations. Let the energy supplied per unit time per unit mass of the system be D_o. The dimensions of this quantity will be

$$D_o = \frac{mv^2}{mt} = \left[\frac{l^2}{t^3}\right],$$

where m = mass, t = time, l = length.

The spectral-energy density of the system must be a function of this energy inflow and of some other variables. If the system does not exhibit any typical dimensions and if its extension in all directions is assumed to be infinite (as holds for the sea or the air above the ground, or for the boundary layer in comparison to the small-scale turbulence), the only general variable that can be introduced is the space-Fourier wave-number κ of the property (temperature, velocity, density, or height of the sea waves) we are interested in. We may therefore assume that the spectral energy density $E(\kappa)$ referred to unit wave-number interval is given by a function of the energy in flow and the space-wave-number: $E(\kappa)$ has the dimensions

$$E(\kappa) = \frac{m\ v^2}{m\ 2\pi/l} = \left[\frac{l^3}{t^2}\right].$$

If this function is written in the form

$$f(D_o, \kappa) = D_o^n \kappa^m = \left(\frac{l^2}{t^3}\right)^n l^{-m},$$

the following dimensional equation results:

$$E(D_o, \kappa) = \frac{l^3}{t^2} = \frac{l^{2n-m}}{t^{3m}}.$$

Comparison of the components left and right yields $m = 2/3$, $m = -5/3$. $E(D_o, \kappa)$ is therefore necessarily of the form

$$E(D_o, \kappa) = D_o^{2/3} \kappa^{-5/3} \cdot \text{constant}.$$

Since the energy flow D_o is independent of the properties of the system and in particular of the space-wave lengths in this system, the spectral intensity decreases as $\kappa^{-5/3}$ with increasing wave-number (decreasing patch size). For the case of homogeneous turbulence, this law was derived by Kolmogorov in 1941 and by von Weizsâckor independently in 1948. The derivation shows that the nature of this law is very general and that it applies to many other phenomena that have no relation to turbulence.

Kraichnan (4) has shown that this classical derivation of the Kolmogorov equilibrium law is not rigorous; and he has derived an improved distribution law on the ground of statistical mechanics. His result is

$$E(\kappa) = \text{const} \cdot \kappa^{-3/2}.$$

In practical cases, the difference between the two laws is very small; and which of the two is used makes very little difference.

Appendix B

THE BERNOULLI EQUATION FOR SMALL-SCALE MOTION

The Euler equation

$$-\frac{1}{\rho} \text{grad } p = \frac{\partial \bar{v}}{\partial t} + \frac{1}{2} \text{grad } v^2 - \text{curl } \bar{v} \times \bar{v}$$

can be integrated along any given path as follows:

$$\frac{p}{\rho} + \frac{v^2}{2} = \text{const.} - \int \frac{\partial \bar{v}}{\partial t} d\bar{s} - \int \text{curl } \bar{v} \times \bar{v} \, d\bar{s}.$$

We now introduce the very plausible assumptions that the decay time of the turbulence is large in comparison to the period of the frequency of interest and that the building-up time of the turbulence is small in comparison to the decay time. The flow may then be considered to be steady ($\partial \bar{v}/\partial t = 0$) when viewed from a coordinate system carried along by the mean flow ($\bar{v} = \bar{v}_o + \bar{v}' = \bar{v}''$. since $\bar{v}_o = 0$), and the above equation simplifies to

$$\frac{p}{\rho} + \frac{v^2}{2} = \text{const} - \int \text{curl } \bar{v} \times \bar{v} \, d\bar{s}.$$

Curl $\bar{v}$ can be expressed by the angular velocity curl $\bar{v} = 2\omega$; and, since we are interested only in patches of turbulence,

$$v \cong a\omega ,$$

where a is the patch radius (or the correlation distance of the velocity fluctuation). To find the acoustic effect of the noise of the pressure fluctuations, we are interested only in small-scale turbulence distributed over a very small region. For a small region the flow may be considered always to be two-dimensional. For a two-dimensional flow, $\bar{v}$ is perpendicular to curl $\bar{v}$ and

$$\frac{p}{\rho} + \frac{v'^2}{2} = \text{const} - 2a \int \omega^2 \, ds .$$

The maximum value of the integral will result when ds is equal to the patch radius a; this maximum is therefore of the same order of magnitude as

$$\pm 2\, a\, \omega^2 = \pm 2v'^2 \approx 2v^{*2} ,$$

where $v' = v^*$ is the fluctuating velocity because of the turbulence. On the average, therefore,

$$p/\rho \cong \pm 2v^{*2} + v^*/2 \cong 2v^{*2} ,$$

and the result reduces to the standardized Bernoulli equation except that the numerical factor is slightly different

$$p/\rho = 2v^{*2} + \text{const}.$$

The above estimate gives an indication of the order of magnitude of the maximum pressure fluctuation. The average pressure fluctuations will probably be about ten times smaller. In this estimate the effect of the velocity gradient in the boundary layer has been neglected. Because of this gradient, the patches are continuously deformed and the motion is no longer stationary. Additional forces are set up that produce considerable fluctuations in pressure. Kraichnan (4b,c) derived the theory for this case on the assumption of a Gaussian velocity correlation. He obtained a similar equation; but the numerical constant now is of the order of magnitude 7:

$$p/\rho = 7\, v^{*2} .$$

REFERENCES

1. Schlichting, H., "Boundary Layer Theory," New York:McGraw-Hill Book Co., 1955

2. Theodorsen, T. and Regier, A., "Experiments on Drag of Revolving Disks, Cylinders, and Streamline Rods at High Speeds," NACA, Report No. 793, 1945

3. Lindgreen, E., "The Transition Process and Other Phenomena in Viscous Flow," Arkov for Fysik, Stockholm, 12:1-169 (1957)

4. (a) Kraichnan, R.H., "Statistical Mechanics of Stationary Homogeneous Hydrodynamic Turbulence," New York University, Research Report No. MH-7, Contract N. AF 19(604)2138, April 1957

   (b) "Pressure Field Within Homogeneous Antistropic Turbulence," J. Acoust. Soc. Am. 28(No. 1):64-72 (January 1956)

(c) "Pressure Fluctuations in Turbulent Flow Over a Flat Plate," J. Acoust. Soc. Am. 28(No. 3):378-390 (May 1956)

(d) "Noise Transmission from the Turbulent Boundary Layer," J. Acoust. Soc. Am. 29:65 (1957)

5. Nikuradse, J., "Untersuchung ueber die Geschwindigkeitsverteilung in turbulenten Stroemungen," VDI Forschungsheft, No. 281, Berlin, 1926

6. (a) Wieselsberger, C., "Reports on the Aerod," Versuchsanstalt Göttingen, I, series, 120-126, 1921

(b) Gebers, F., Schiffbau, 9:435, 475 (1908); also Schiffbau, 22 (1919)

(c) Schoenherr, K.E., "Resistance of Flat Surfaces Moving Through a Fluid," Trans. Soc. Nav. Arch. and Mar. Engrs. 40:279 (1932)

(d) Kempf, G., "Neue Ergebnisse der Widerstandsforschung," Werft, Reederei, Hafen, 10:234, 247 (1929)

(e) Nikuradse, J., "Turbulente Reibungsschichten an der Platte," Munich:R. Oldenbourg, 1942

(f) Kempf, G., "Uber den Einfluss der Rauhigkeit auf den Widerstand von Schiffen," Jahrb. d. Schiffbautechn. Gessellschaft, 38:159, 233 (1937); and "The Effect of Roughness on the Resistance of Ships," Engineering, London, 143:417 (1937), see also Trans. Inst. Nav. Architects, 79, 109, and 137, 1937.

7. Laufer, J., "Investigation of Turbulent Flow in a Two-Dimensional Channel," NACA, Report V. 1053, 1951

8. Harrison, Mark, "Correlation and Spectra of Pressure Fluctuations on the Wall Adjacent to a Turbulent Boundary Layer," J. Acoust. Soc. Am. 29:1252A, 1957

9. Goldstein, M., "A Note on Roughness, A.R.U., Report and Memo No. 1763, 1936

10. Kolmogorov, A.N., "The Local Structure of Turbulence in Incompressible Viscous Fluid for very Large Reynolds' Numbers," C. R. Acad. Sci. U.R.S.S. 30:301 (1941)

11. Kolmogorov, A.N., "Dissipation of Energy in the Locally Isotropic Turbulence," C. R. Acad. Sci. U.R.S.S. 32:16 (1941)

* * * * *

DISCUSSION

R. H. Kraichnan (New York University)

I should like to ask if when you go through the transition in which the roughnesses push up through the laminar sublayer you observe the same proportionality between drag and noise. Also, I should like to express a doubt that the $k^{-5/3}$ behavior which you observe has much relevance to inertial range phenomena. Actually, the inertial range law for pressure which might reasonably be expected on the basis of the Kolmogorov theory is approximately κ^{-2}, or steeper. My guess would be that the pressure fluctuations which you observe at high frequencies arise not from the fine structure of the outer part of the boundary-layer (where an inertial range might perhaps be expected) but from the intensely-sheared dissipation layer just above the laminar sublayer.

E. Meyer (Physikalisches Institüt der Universität Göttingen)

In connection with the very interesting statements of Dr. Skudrzyk I would like to report on some experiments dealing with "noise of streaming water" which were carried out in our institute in Göttingen by Mr. Dinkelacker.

The characteristic feature of the experiments is the simplicity of the apparatus (Fig. 1). Water from the water mains streams through the test tube with an adjustable velocity. The walls of the test tube may consist of different materials (in Fig. D1 a glass tube is shown). The inner surface of the tubes can be treated to give different degrees of roughness. Having passed the test tubes, the water is collected in a storage tank. The test tube is connected to the water mains by means of a long rubber tube. This rubber tube works as an acoustic wave guide below its cut-off frequency, thus separating the test tube from the mains with respect to structure-borne sound. The measurements are carried out with a structure-borne sound microphone attached to the outside of the test tube. The frequency response of the set-up including the test tube can be determined.

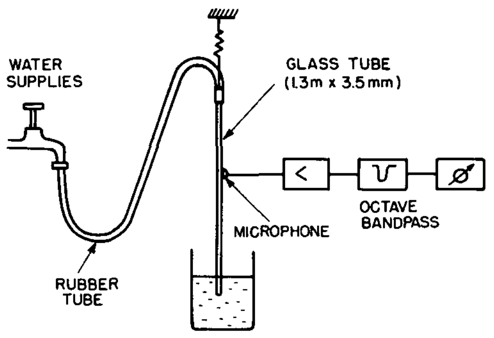

Fig. D1 - Noise of streaming water in a tube (arrangement)

In Fig. D2 the sound level of octave bands is plotted against the frequency with the stream velocity as a parameter. It is obvious from the diagram that the maximum of the sound intensity shifts to higher frequencies with rising stream velocity.

These relations are more clearly visible in Fig. D3, where the same results are plotted, but with the stream velocity as abscissa and the octave ranges as parameter. The onset of the noise is given when, with rising streaming velocity the Reynolds number is approximately reached. In the beginning, most of the noise is concentrated on the lowest octave band. For the higher octave bands the point of onset shifts to higher stream velocities.

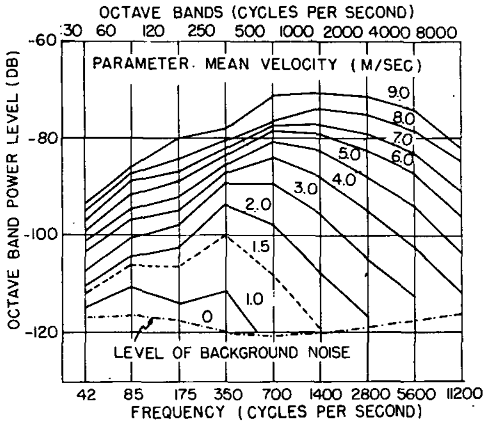

Fig. D2 - Noise of streaming water in a tube of glass

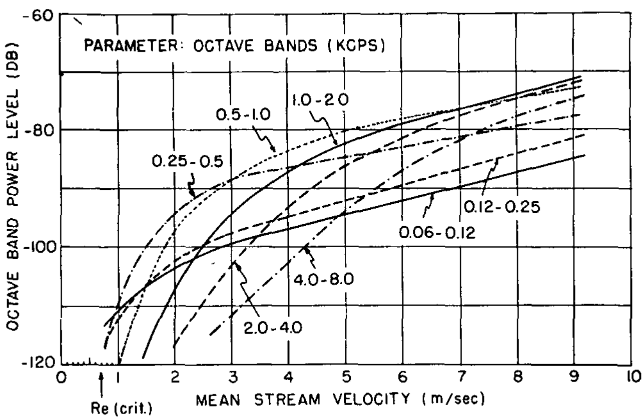

Fig. D3 - Noise of streaming water in a tube of glass

These preliminary results seem to indicate that the turbulence patches have smaller dimensions at higher velocity.

E. Skudrzyk

With regard to the drag-noise ratio: the extrapolation is very hypothetical but is somewhat in agreement with experimental results. As long as nothing better is available we feel we should stick to that.

Of course the spectrum interpolation is again highly hypothetical and the only thing I am really allowed to admit is that the experimental results do not contradict our theoretical concept at the moment.

* * * * *